Enhancement of bulklike second-order nonlinear susceptibility in SiGe/Si step wells and biasing-field controlled $(Si_5Ge_5)_{100}$ superlattices

Xinhui Zhang, Zhenghao Chen,* Linzhen Xuan, Shaohua Pan, and Guozhen Yang
Laboratory of Optical Physics, Institute of Physics & Center for Condensed Matter Physics, Chinese Academy of Sciences, P.O. Box 603, Beijing 100080, People's Republic of China

(Received 14 May 1997; revised manuscript received 25 August 1997)

Second-harmonic generation (SHG) from electric-field biased $(Si_5Ge_5)_{100}$ superlattices and $Si_{0.75}Ge_{0.25}/Si_{0.57}Ge_{0.43}/Si$ step asymmetry wells were studied. Contributions from the different sources to second-order susceptibility $\chi^{(2)}$ were systematically analyzed for these two kinds of asymmetry Si/Ge quantum-well structures. The bulklike $\chi^{(2)}$ was large enough to be observed while the strain-induced contribution to $\chi^{(2)}$ was relatively small for $(Si_5Ge_5)_{100}$ superlattices under an applied field of 100 kV/cm. However, strain-enhanced effects were large compared to the contribution from the bulk for the optical $\chi^{(2)}$ in SiGe/Si step wells. The results show that different asymmetric structures have different contributional distributions of SHG sources. The peak value of $\chi^{(2)}$ was as large as 5×10^{-6} esu for a $(Si_5Ge_5)_{100}$ superlattice under 100 kV/cm electric field and 0.6×10^{-6} esu for SiGe/Si step wells. These large bulklike $\chi^{(2)}$ values indicate that Si/Ge quantum wells with asymmetric structures have potential applications to optoelectronic materials and devices with the existing Si-based technology. [S0163-1829(97)01448-3]

I. INTRODUCTION

Larger optical nonlinearities, especially second-order nonlinear effects, arising from semiconductor heterojunctions and quantum wells, together with their possible related optoelectronic device applications, have received a great deal of interest in recent years. The advantage that Si/Ge superlattices (SL's) and multiple quantum wells can be easily integrated with matured Si-based technology drives intensive studies for optical properties such as second-harmonic generation (SHG) of Si/Ge systems. Unfortunately, the indirect nature of the fundamental band gap of Si/Ge systems prevents their use as an important optoelectronic material in the future. Furthermore, for centrosymmetric materials, such as single-crystal Si or Ge, bulk SHG is forbidden within the electric dipole approximation. However, short-period Si_mGe_n strained superlattices have attracted considerable research attention because they offer the possibility of fundamental changes in linear and nonlinear optical properties of group-IV semiconductors.[1,2] In particular, it was predicted, at least theoretically, that there exists a large second-order nonlinear susceptibility $\chi^{(2)}$ for Si_mGe_n if m and n are both odd.[3–5] But such predicted large bulk dipole allowed (BDA) SHG was never observed, which was attributed to the incapability of precise control of layer thickness in superlattices in present molecular-beam epitaxy (MBF).[6,7]

In addition to BDA $\chi^{(2)}$ source, it was demonstrated that weak SHG from Si_mGe_n SL's can still arise from interface strain-induced mechanisms[10–12] and from bulk electric quadruple sources.[8,9] One can observe the azimuthal angle dependence of the output SHG intensities with a certain polarization arrangement to determine the difference of these SHG sources. On the other hand, it is known that using a built-in asymmetric structure, such as graded wells or coupled asymmetric wells, or a symmetric quantum well with an external applied electric field, a large BDA second-order susceptibility becomes possible.[13–15] However, except for second-harmonic generation research in intersubband transitions of p-doped asymmetric SiGe/Si quantum wells,[16,17] to our knowledge, no research on optical second-order susceptibility from interband transitions in SiGe/Si asymmetric step wells and in Si/Ge superlattices system with a biasing electric field were reported.

In this paper, a thicker $(Si_5Ge_5)_{100}$ superlattice with $Si_{0.5}Ge_{0.5}$ substrate suggested by Turton and Jaros[18] was designed as the first sample, which was predicted to have direct transition properties and the largest oscillator strength across the band gap. Therefore, we expect that such a thicker $(Si_5Ge_5)_{100}$ superlattice, when strong enough external applied electric field is added to break the inversion symmetry, should have advantage for SHG, especially for BDA source observation. We have made a systematic study on such a biased $(Si_5Ge_5)_{100}$ superlattice to show trends of SHG with biasing field. Moreover, since the asymmetry of electronic wave functions of the above system is mainly induced by the applied electric field, it is worth comparing the SHG of such a system with that of an asymmetric quantum-well structure of Si/Ge, in which the asymmetry of electronic wave functions is mainly due to structure asymmetry itself. For the asymmetric quantum-well structure, we chose SiGe/Si step wells as our second sample. We made a comparison of optical $\chi^{(2)}$ of interband transitions in the two samples, i.e., SiGe/Si step wells and biasing field controlled $(Si_5Ge_5)_{100}$ superlattice. In particular, different contributions of optical $\chi^{(2)}$, such as BDA source, interfaces, strain-induced mechanisms, and bulk electric quadruple source, were analyzed for the two samples. The results show that the relative importance between these $\chi^{(2)}$ sources in the first sample is obviously different from that in the second one. The remainder of this paper is organized as follows. The material growth and quality of the two kinds of samples are described in Sec. II. The measurements and analysis of $\chi^{(2)}$ are given in Sec. III. Section IV gives short conclusions.

0163-1829/97/56(24)/15842(5)/$10.00 © 1997 The American Physical Society

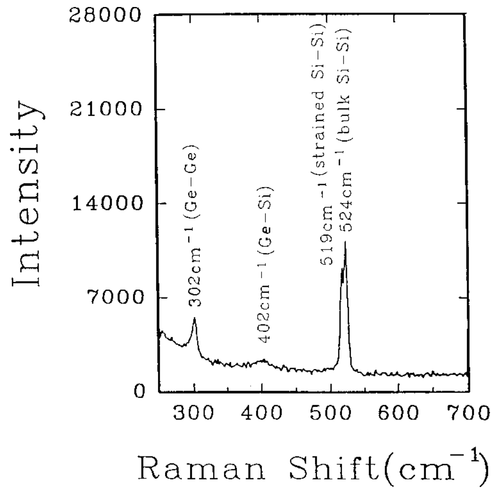

FIG. 1. Raman spectrum of the $(Si_5Ge_5)_{100}$ sample with the excitation of 514.5 nm by using Ar^+ laser in the back-scattering geometry.

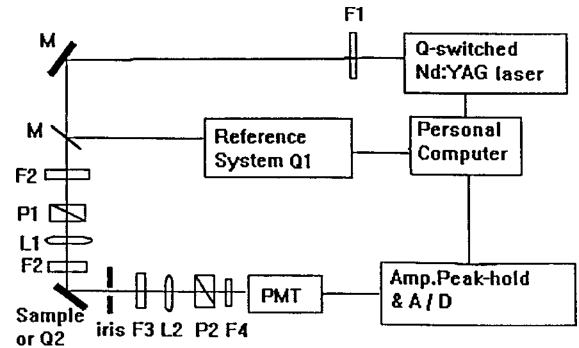

FIG. 2. The block diagram of the experimental setup: F_1 and F_2, infrared filter (0.59–2.0 μm); F_3, interference filter (5240–5440 Å); F_4, $CuSO_4$ filter (5-cm cell); L_i, lens; P_i, polarizer; PMT, photomultiplier tube.

II. EXPERIMENT

A. Samples

The first sample used was p-doped 100 periods of $(Si_5Ge_5)_{100}$ superlattice. The buffer layers consisted of 2000-Å-thick Si and 500-Å-thick $Si_{0.5}Ge_{0.5}$ with boron-doping concentration of 4×10^{18} cm^{-3}. On top of the $(Si_5Ge_5)_{100}$ superlattice, a boron-doped $Si_{0.5}Ge_{0.5}$ with thickness of 500 Å was grown and followed by a 500 Å Si cap layer with boron-doping concentration of 4×10^{18} cm^{-3}. Figure 1 exhibits the measured Raman spectrum result of our MBE-grown sample 1. The measurement was made using an Ar ion laser (514.5 nm) in the back-scattering geometry. The shapes of these Raman features show rather good broadness and symmetry that indicate the better crystalline quality of our sample 1. In order to measure the electric-field controlled $\chi^{(2)}$, sample 1 was first processed using the standard photolithographic method into 7×7-mm^2, 0.4-μm-deep mesas. All Ohmic contacts were made on the etched p-doped cap and buffer layers with a real measured area of 5×5 mm^2 left. The sample was mounted using Ag wires to provide the electrical connections in order to add a perpendicular field across the superlattice. The second sample used was asymmetric step wells: the 20 periods of strained multiple quantum-well structure, each step well consisting of a 36-Å $Si_{0.75}Ge_{0.25}$ step, 19-Å $Si_{0.57}Ge_{0.43}$ well, and 200-Å undoped Si barrier. The sample was p-doped in the SiGe wells with boron-doping concentration of 4×10^{18} cm^{-3}. The 1500-Å Si buffer and 500-Å Si cap layers were also p-doped with concentration of 4×10^{18} cm^{-3}. The x-ray diffraction (XRD) spectrum was used to analyze the composition and the MBE grown quality. XRD indicated that there was some disorder of the SiGe/Si step wells which leads to a reduction of Bragg reflected strength of the diffraction peaks of the $Si_{0.75}Ge_{0.25}/Si_{0.57}Ge_{0.43}$ wells comparing with the peak of the Si substrate.

B. Experimental setup

The reflected measurements of SHG from the two samples were taken using a pulsed Q-switched yttrium aluminum garnet (YAG) laser. The experimental arrangement is shown by Fig. 2. The fundamental beam of 1.06 μm was s or p polarized with an incident angle of 45°, which was separated into two parts. One beam was directed through the Z-cut quartz crystal Q_1, which generated the second harmonic used for normalization against possible laser fluctuations. The other beam was used to generate second harmonic by reflection from either the sample or a Z-cut quartz Q_2. The second-harmonic signal from this quartz Q_2 was needed for calibration of the nonlinear susceptibility of the sample. The p-polarized component of reflective SH light at 532 nm was measured as a function of the sample azimuthal angle. Each measured datum was obtained by a photomultiplier tube and by averaging the results of 100 laser shots using an instantaneous recorder-computer system.

III. RESULTS AND DISCUSSION

First, we measured the infrared-absorption spectra for our two samples by a Bio-Rad Fourier-transform infrared spectrometer at room temperature, from which we obtained that the band-gap energy of the $(Si_5Ge_5)_{100}$ superlattice without biasing field is $E_g\approx0.99$ eV, and the band-gap energy of the $Si_{0.75}Ge_{0.25}/Si_{0.57}Ge_{0.43}$ step wells is $E_g\approx0.97$ eV. Hence, the laser wavelength (1.06 μm, or photon energy 1.18 eV) we chose could guarantee interband transitions at off-resonant conditions for both samples. Since the main purpose of the present paper is to analyze and compare the different $\chi^{(2)}$ sources of interband transitions for the two kinds of asymmetric Si/Ge systems, our choice of the excitation wavelength (1.06 μm) should be suitable because the off-resonant conditions could simplify the physics problem we study.

Second, we measured the SHG from the $(Ge_5Si_5)_{100}$ superlattice under different applied electric fields to observe the trends of SHG with biasing field. In Fig. 3, we show the results of electric-field controlled SHG under ten different biasing field strengths. It is indicated that the SHG increases rapidly with E for $E\leqslant100$ kV/cm, while for larger external field E, there is little increase of the SHG. The reasonable explanation is given as follows: First, like the calculation of second-harmonic coefficient $\chi^{(2)}$ in a biased p-type quantum well by Tsang and Chuang,[19] for small biasing field E, larger E will create stronger asymmetry, and hence a resulting larger $\chi^{(2)}$. However, for very large biasing fields, the

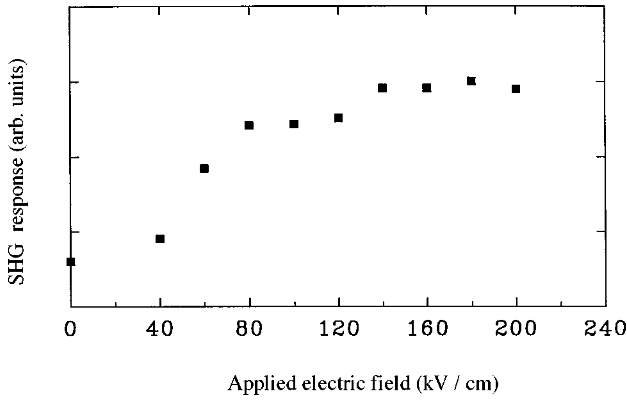

FIG. 3. Second-harmonic generation response is plotted versus the biasing electric fields for $(Si_5Ge_5)_{100}$ superlattice.

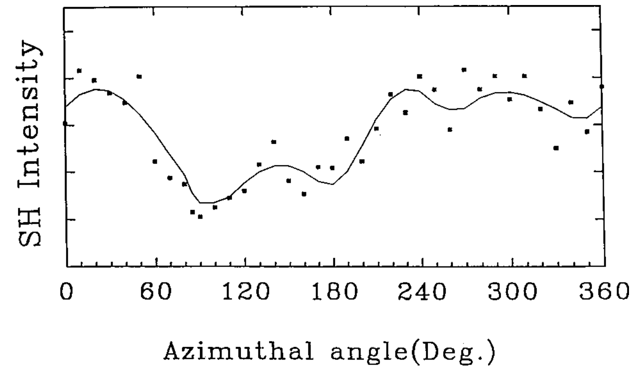

FIG. 5. $I_{p,p}^{(2\omega)}(\psi)$ from the step asymmetric wells. The solid curve is a best fit using Eq. (2).

asymmetry has already been maximized so that a further increase of E no longer increases $\chi^{(2)}$. Second, the second-order susceptibility $\chi^{(2)}$ is proportional to the optical matrix element of the lowest energy transition across the band gap, which is actually enhanced rapidly with a small external electric field E and is reduced when $E \geqslant 100$ kV/cm, and the reduction rate for a $(Si_5Ge_5)_n$ system with a larger n $(=13)$ is less than that with $n=9$.[20] In our case of $(Si_5Ge_5)_{100}$ structure shown by Fig. 3, a similar trend is seen for SHG with biasing field. In particular, when biasing electric field is larger than 100 kV/cm, the optical SHG begins to decay slowly. It might be, at the same time, there are also no further increased asymmetry with strong biasing field. Meanwhile, the redshifted band gap is much farther away from the resonance energy with incident light when the electric field increases. These effects, in average, result in little change of $\chi^{(2)}$ when the biasing field is larger than 100 kV/cm. In brief, here we emphasize that the rapid increase of SHG is mainly because of the broken inversion symmetry of the superlattice caused by external applied electric field. Therefore, we suggest that there exists a large BDA $\chi^{(2)}$ source in $(Si_5Ge_5)_{100}$ superlattice with a enough strong biasing field.

Third, we analyzed and compared with the different contributions of second-order susceptibility $\chi^{(2)}$ coming from BDA source, interfaces, strain-induced mechanism, and bulk electric quadruple source in the two different kinds of asymmetric systems, namely, $(Si_5Ge_5)_{100}$ superlattice with a fixed strong biasing field and SiGe/Si step wells with compositional asymmetric structure.

To distinguish the SHG sources of the sample, the harmonic signal was measured as a function of sample azimuthal angle ψ. For SL's grown on Si(001) substrates, the p-polarized SH intensity can be expressed as a function of ψ in the form of[7]

$$I_{g,p}^{(2\omega)}(\psi) \propto \left| \sum_{m=0}^{4} c_{g,p}^{(m)} \cos(m\psi) \right|^2, \tag{1}$$

where ψ is the angle between the plane of incidence and the Si[110] direction, and g is the fundamental polarization light (s or p). As it is known, the complex Fourier coefficients $c_{g,p}^{(m)}$ with different m represent the contributions from different SHG sources:[21,22] the $c^{(0)}$ coefficient, which leads to an isotropic response, mainly arises from strain-enhanced interface effect; the $c^{(1)}$ and $c^{(3)}$ coefficients are due to the miscutting of the substrate which preserve a C_{1v} surface symmetry; the $c^{(4)}$ coefficient results from bulk quadruple sources; $c_{(g,p)}^{(2)}$ should be large and dominate the other terms if there exists BDA $\chi^{(2)}$ in the sample. Figure 4 shows $I_{s,p}^{(2\omega)}(\psi)$ trace with azimuthal angle ψ for the $(Si_5Ge_5)_{100}$ superlattice (the first sample) under external electric field of 100 kV/cm. We noticed that our sample 1 has the similar $(Si_5Ge_5)_n$ structure with that in Ref. 6. However, the applied external field distorted the original structure of sample 1; therefore it is seen from Fig. 4 that the symmetry properties revealed by the azimuthal angle dependency of SHG for an applied field biased $(Si_5Ge_5)_{100}$ superlattice have complex changes compared to that of $(Si_5Ge_5)_n$ without biasing field.[6] Figure 5 gives $I_{p,p}^{(2\omega)}(\psi)$ obtained from the step asymmetric wells (the second sample).

In order to give a best fit for the experimental data of SH intensities, a more general form of truncated Fourier expansion in ψ for SH generation from noncentrosymmetric cubic faces given by Bottomley *et al.*[23] was used:

$$I^{(2\omega)}(\psi) \propto \left| \sum_{m=0}^{4} [a^{(m)} \cos(m\psi) + b^{(m)} \sin(m\psi)] \right|^2. \tag{2}$$

The best fits are shown by the solid curves in Figs. 4 and 5, and the related Fourier coefficients $c^{(m)}$ are listed in Table I. Note that in Table I and in the following $c^{(m)}$ is defined as $c^{(m)} = a^{(m)2} + b^{(m)2}$, the same as in Ref. 23. As pointed in Ref. 7, such fitting results by Fourier analysis are not unique. We found, for $|C_{sp}^{(2)}|$, the relative value can range from 0.82 to 1. Here, we give the best fits.

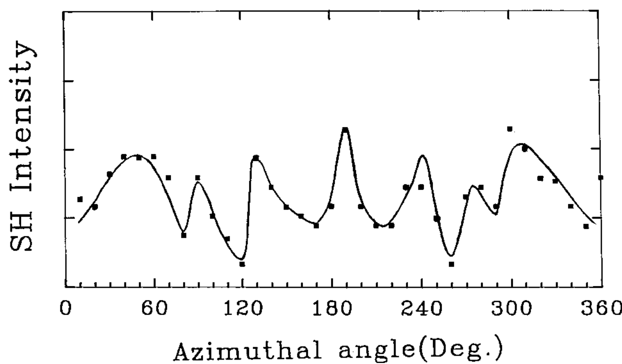

FIG. 4. $I_{s,p}^{(2\omega)}(\psi)$ from the $(Si_5Ge_5)_{100}$ SL with an applied field of 100 kV/cm. The solid curve is a best fit using Eq. (2).

TABLE I. Fourier coefficients of $c^{(m)}$ in the SH field $E^{(2\omega)}$ (ψ) obtained from intensity data for the two samples, normalized to the largest $c^{(m)}$ for each case. (As pointed out in Ref. 7, such fitting results by Fourier analysis are not unique. We found, for $|C_{sp}^{(2)}|$, the relative value can range from 0.82 to 1.)

Samples	$c^{(0)}$	$c^{(1)}$	$c^{(2)}$	$c^{(3)}$	$c^{(4)}$
$(Si_5Ge_5)_{100}$ (s,p) (applied field of 100 kV/cm)	0.05	0.36	1	0.36	0.02
SiGe/Si step well (p,p)	1	0.26	0.28	0.02	0

It is shown in Table I that $c_{s,p}^{(2)}$ is the largest and $c_{s,p}^{(0)}$ is relatively very small for the biasing field of 100 kV/cm controlled $(Si_5Ge_5)_{100}$ superlattice, which means that a large bulk dipole allowed SHG can indeed be observed in our thicker $(Si_5Ge_5)_{100}$ superlattice when an electric field of 100 kV/cm is applied, while the SHG response from strain-induced effect is very little for the thicker $(Si_5Ge_5)_{100}$ superlattice. Maybe, that is because the strain stress was almost relaxed for our symmetry-strained sample by using an alloy buffer layer $Si_{0.5}Ge_{0.5}$ (500 Å) in order to obtain a thicker $(Si_5Ge_5)_{100}$ superlattice. However, $c_{s,p}^{(0)}$ dominates the others for the $Si_{0.75}Ge_{0.25}/Si_{0.57}Ge_{0.43}/Si$ step wells, which implies that the strain-enhanced effect is the main contribution to SH signal for the SiGe/Si step wells. It suggests that, comparing with the $(Si_5Ge_5)_{100}$ sample, more complex interfaces and stronger strain situation exist in the $(SiGe/Si)_{20}$ step wells. Also one can see from Table I that the value of $c^{(2)}$, which is attributed to BDA $\chi^{(2)}$, is the second largest $c^{(m)}$ for the SiGe/Si step well sample. Moreover, Table I shows that, for the two different asymmetric structures, the $c^{(4)}$ terms are very small which means that the bulk quadruple source for SHG can be neglected.

For an s-polarized incident beam, the p-polarized SH output field in reflection from a surface can be calculated as[24]

$$E_p(2\omega)=\frac{\varepsilon 2\pi k_1^2(2\omega)}{\varepsilon_1(2\omega)k_{1z}(2\omega)}\left[\frac{k_{1z}(2\omega)}{k_1(2\omega)}\times L_{xx}(2\omega)L_{yy}(\omega)L_{yy}(\omega)\chi^{(2)}_{s,xyy}\right]E_1^2(\omega)+\frac{\varepsilon 2\pi k_1^2(2\omega)}{\varepsilon_1(2\omega)k_{1z}}\left[\frac{k_{1x}(2\omega)}{k_1(2\omega)}\times L_{zz}(2\omega)L_{yy}(\omega)L_{yy}(\omega)\chi^{(2)}_{s,zyy}\right]E_1^2(\omega)(2\omega), \quad (3)$$

where k is the wave vector of the beam and $E_I(\omega)$ is the strength of incident field. L_{ii} $(i=x,y,z)$ is the Fresnel factor. To relate the effective susceptibility in the laboratory frame with special $\chi^{(2)}$ components fixed in the sample frame, one should perform transformation between the two coordinates.[21,23] This results in an angle dependence of the output SH field as shown in Eq. (1).

It is known that the refractive index values of Si and Ge are $n_{Si}(\omega)=3.54$, $n_{Si}(2\omega)=4.10$, $n_{Ge}(\omega)=4.40$, and $n_{Ge}(2\omega)=5.02$.[26] On average we choose $n(\omega)=3.97$ and $n(2\omega)=4.56$ for the $(Si_5Ge_5)_{100}$ superlattice and $n(\omega)=3.76$ and $n(2\omega)=4.73$ for the step wells. These values are used to calculate the Fresnel factors using the method studied by Lüpke, Bottomley, and Van Driel.[21] Then, Eq. (3) and the Fourier coefficients $c^{(m)}$ are used to evaluate the numerical values of $\chi^{(2)}$ corresponding to different SH sources, and the $\chi^{(2)}$ values were calibrated by quartz $\chi^{(2)}_{111}$ of 1.9×10^{-9} esu.[25] The results are summarized in Table II.

TABLE II. Numerical calculation results of SH susceptibility $\chi^{(2)}$ related to different SH sources from the $(Si_5Ge_5)_{100}$ Sl with s(in)-p(out) combination and applied field of 100 kV/cm, calibrated with a Z-cut quartz ($\chi^{(2)}_{111}=1.9\times10^{-9}$ esu).

SH source	related effective $\chi^{(2)}$ (esu)
strain-enhanced effect	1.6×10^{-7}
BDA mechanism	5.0×10^{-6}
miscutting interfaces effect	4.8×10^{-7}
bulk quadruple contribution	8.8×10^{-8}

The evaluated values of SH susceptibility $\chi^{(2)}$ for our two samples have been compared with other results of experimental and theoretical researches for SiGe/Si systems. These comparisons are listed in Table III. It can be seen from Table III that the peak value of $\chi^{(2)}$ for electric-field controlled $(Si_5Ge_5)_{100}$ Sl is one order of magnitude larger than the theoretical prediction by Ghahranmani, Mass, and Sipe.[4] Moreover, the SH generation for the $(Si_5Ge_5)_{100}$ SL with an external electric field of 100 kV/cm can be comparable with the SiGe/Si step wells. The measured large $\chi^{(2)}$ indicates that the two kinds of asymmetric structures, namely, the Si_mGe_n superlattices and the SiGe/Si step wells, have strong potential applications to the future important optoelectronic devices combined with the existing Si-based technology.

IV. CONCLUSIONS

Second-harmonic generation from electric-field biased $(Si_5Ge_5)_{100}$ superlattices and $Si_{0.75}Ge_{0.25}/Si_{0.57}Ge_{0.43}/Si$

TABLE III. Numerically calculated $\chi^{(2)}$ of the present study comparing with the other research works.

Samples	$\chi^{(2)}$ (esu)
$(Si_5Ge_6)_{100}$ with applied field of 100 kV/cm (this paper)	5.0×10^{-6} (Expt.)
$Si_{0.75}Ge_{0.25}/Si_{0.53}Ge_{0.47}/Si$ step well (this paper)	0.6×10^{-6} (Expt.) (interband transition) (this paper)
$Si_{0.75}Ge_{0.25}/Si_{0.57}Ge_{0.43}/Si$ step well (Ref. 16)	1.2×10^{-6} (Expt.) (intersubband transition) (Ref. 6)
$(Si_5Ge_5)_3$ (Ref. 4)	10^{-7}–10^{-8} (Theor.)

asymmetry step wells was studied. The BDA $\chi^{(2)}$ for the electric-field biased $(Si_5Ge_5)_{100}$ SL is large enough to be observed while SH generation arising from strain-induced effect is relatively very small. However, for the SiGe/Si step wells, strained-enhanced effect is the main contribution to the SH signal compared to the other SH sources. This indicates that different asymmetric structures have different contributional distributions of SHG sources. The numerical calculations of $\chi^{(2)}$ for $(Si_5Ge_5)_{100}$ superlattices and SiGe/Si step wells were made. The evaluated value of $\chi^{(2)}$ is as large as 5×10^{-6} esu for the $(Si_5Ge_5)_{100}$ superlattice under 100 kV/cm electric field and 0.6×10^{-6} esu for the SiGe/Si step wells. The observed large $\chi^{(2)}$ implies that Si/Ge systems with asymmetric structures can become potential optoelectronic materials with the existing Si-based technology.

ACKNOWLEDGMENT

This work was supported by the National Natural Science Foundation of China.

*Electronic address: zhchen@aphy02.iphy.ac.cn

[1] R. People and S. A. Jackson, Phys. Rev. B **36**, 1310 (1987).
[2] H. Presting, H. Kibbel, M. Haros, R. M. Turton, U. Menczigar, G. Abstraiter, and H. G. Grimmeiss, Semicond. Sci. Technol. **7**, 1127 (1992).
[3] ED Ghahranmani, D. J. Moss, and J. E. Sipe, Phys. Rev. Lett. **64**, 2815 (1990).
[4] ED Ghahranmani, D. J. Moss, and J. E. Sipe, Phys. Rev. B **43**, 8990 (1991).
[5] ED Ghahranmani and J. E. Sipe, Appl. Phys. Lett. **62**, 2245 (1993).
[6] D. J. Bottomley, G. Lüpke, M. L. Ledgerwood, X. Q. Zhou, and H. M. Van Driel, Appl. Phys. Lett. **63**, 2324 (1993).
[7] D. J. Bottomley, J. M. Baribeau, and H. M. Van Driel, Phys. Rev. B **50**, 8564 (1994).
[8] H. W. K. Tom, T. F. Heinz, and Y. R. Shen, Phys. Rev. Lett. **51**, 1983 (1983).
[9] J. E. Sipe, D. J. Moss, and H. M. Van Driel, Phys. Rev. B **35**, 1129 (1987).
[10] S. V. Govorkov, V. I. Emel'yano, N. I. Koroteev, G. I. Petrov, I. L. Shumay, and V. V. Yakovlev, J. Opt. Soc. Am. B **6**, 117 (1989).
[11] O. P. Zaitcev, V. I. Mashanov, E. M. Pazhitnov, D. V. Petrov, O. P. Pcheljakov, and V. V. Trifutin, Semicond. Sci. Technol. **8**, 1493 (1993).
[12] Lionel Friedman and Richard A. Sorf, J. Phys. Lett. **61**, 2342 (1987).
[13] M. K. Gurnick and T. A. DeTemple, IEEE J. Quantum Electron. **QE-19**, 791 (1983).
[14] L. Tsuang, D. Ahn, and S. L. Chuang, Appl. Phys. Lett. **52**, 697 (1988).
[15] J. Khurgin, J. Appl. Lett. **64**, 5026 (1988).
[16] M. Seto, M. Helm, Z. Moussa, P. Boucaud, F. H. Julien, J.-M. Lourtioz, J. F. Nützel, and G. Abstreiter, Appl. Phys. Lett. **65**, 2969 (1994).
[17] K. B. Wong, M. J. Shaw, and M. Jaros, Mater. Sci. Eng. B **21**, 296 (1993).
[18] R. J. Turton and M. Jaros, IEE Proc.: Optoelectron. **138**, 323 (1991).
[19] Leung Tsang and Shun-lien Chuang, Appl. Phys. Lett. **60**, 2543 (1992).
[20] J. P. Hagon, R. J. Turton, A. T. Miloszewski, G. S. M. Elfarday, and M. Jaros, Superlattices Microstruct. **16**, 125 (1994).
[21] G. Lüpke, D. J. Bottomeley, and H. M. Van Driel, J. Opt. Soc. Am. B **11**, 33 (1993).
[22] G. Lüpke, D. J. Bottomeley, and H. M. Van Driel, Phys. Rev. B **47**, 10 389 (1993).
[23] D. J. Bottomeley, G. Lüpke, J. G. Mihaychuk, and H. M. Van Driel, J. Appl. Phys. **74**, 6072 (1993).
[24] Y. R. Shen, Annu. Rev. Phys. Chem. **40**, 327 (1989).
[25] Y. R. Shen, *The Principles of Nonlinear Optics* (Wiley, New York, 1984), Chap. 7.
[26] *Semiconductors*, edited by O. Madelung, Landolt-Börnstein, New Series, Group III, Vol. 22, Pt. a (Springer-Verlag, Berlin, 1987), p. 22.